Thermal Treatment of a Keggin-Type Diplatinum(II)-Coordinated Polyoxotungstate: Formation of Hydrophilic Colloidal Particles and Photocatalytic Hydrogen Production

Thermal Treatment of a Keggin-Type Diplatinum(II)-Coordinated Polyoxotungstate: Formation of Hydrophilic Colloidal Particles and Photocatalytic Hydrogen Production

Chika Nozaki Kato,*[a,b] Koki Aono,[a] Akihiro Kurihara,[a] Toshiya Kubota,[a] Ryota Kasai,[a] and Kosuke Suzuki[c]

---

[a] Dr. C. N. Kato, K. Aono, A. Kurihara, T. Kubota, R. Kasai

Department of Chemistry, Faculty of Science, Shizuoka University, 836 Ohya, Suruga-ku, Shizuoka 422-8529, Japan

E-mail: kato.chika@shizuoka.ac.jp

[b] Dr. C. N. Kato

Research Institute of Green Science and Technology, Shizuoka University, 836 Ohya, Suruga-ku, Shizuoka 422-8529, Japan

[c] Dr. K. Suzuki

Department of Applied Chemistry, School of Engineering, The University of Tokyo, 7-3-1 Hongo, Bunkyo-ku, Tokyo 113-8656, Japan

Abstract: Hydrophilic platinum-polyoxotungstate colloidal particles formed by a self-assembly of $Cs_4[\{Pt(OH)_2\}_2 \cdot SiW_{12}O_{40}]$ were successfully obtained by calcining a cesium salt of α-Keggin-type diplatinum(II)-coordinated silicotungstate, $Cs_4[\alpha\text{-}SiW_{11}O_{39}\{cis\text{-}Pt^{II}(NH_3)_2\}_2] \cdot 11H_2O$ (**Cs-Si-Pt**), in air at 300 °C. During the thermal treatment, the structure of the mono-lacunary Keggin-type silicotungstate ligand $\{SiW_{11}O_{39}\}$ transformed to that of $\{SiW_{12}O_{40}\}$, and the diplatinum sites in **Cs-Si-Pt** transformed to the platinum hydroxides with the elimination of the ammonia molecules coordinated to the platinum sites. All four cesium ions in $Cs_4[\{Pt(OH)_2\}_2 \cdot SiW_{12}O_{40}]$ could be ion-exchanged by four tetramethylammonium ions, and hydrophilic $[(CH_3)_4N]_4[\{Pt(OH)_2\}_2 \cdot SiW_{12}O_{40}]$ colloidal particles were also formed in aqueous solution. The calcined sample acted as a photocatalyst for hydrogen evolution from aqueous triethanolamine (TEOA) under visible light irradiation ($\lambda = \geq 440$ nm) in the presence of Eosin Y, $K_5[\alpha\text{-}SiW_{11}\{Al(OH_2)\}O_{39}] \cdot 7H_2O$, and titanium dioxide. Although relatively rapid deactivation was observed, the turnover frequency was 3588 h^{-1} after 20 min, and the turnover number exceeded 4600 after 3 h of light irradiation.

Keywords: polyoxometalate; platinum; air-calcination; self-assembly; hydrogen production

Introduction

Photocatalysts for hydrogen production from water have received much attention because hydrogen is critical for the construction of a clean-energy society.[1–3] Among the various photocatalysts that have been developed so far, platinum is often used as a co-catalyst for constructing photocatalytic systems that produce hydrogen.[4] However, platinum is expensive and has a low abundance; thus, its practical use is limited. Therefore, further improvement of the platinum utilization efficiency is a significant research goal.

Polyoxometalates (POMs) are metal-oxygen clusters with enormously diverse chemical structures and physical properties, and they are expected to have applications in catalytic, magnetic, electrical, and optical materials.[5–8] One method for enhancing the functionality of POMs is to introduce metal species into the vacant site(s) of lacunary POMs. Several structurally well-defined Pt^{2+}-containing POMs, e.g., $[Pt_2(W_5O_{18})_2]^{8-}$,[9] $[anti\text{-}Pt_2(\alpha\text{-}PW_{11}O_{39})_2]^{10-}$,[10] and $[syn\text{-}Pt_2(\alpha\text{-}PW_{11}O_{39})_2]^{10-}$,[10] have been reported. In the last few years, we have also synthesized cesium and tetramethylammonium salts of α-Keggin diplatinum(II)-coordinated phospho-, silico-, and germanotungstates, including $Cs_3[\alpha\text{-}PW_{11}O_{39}\{cis\text{-}Pt(NH_3)_2\}_2]\cdot 8H_2O$, $[(CH_3)_4N]_3[\alpha\text{-}PW_{11}O_{39}\{cis\text{-}Pt(NH_3)_2\}_2]\cdot 10H_2O$, $[(CH_3)_4N]_4[\alpha\text{-}SiW_{11}O_{39}\{cis\text{-}Pt(NH_3)_2\}_2]\cdot 13H_2O$, and $[(CH_3)_4N]_4[\alpha\text{-}GeW_{11}O_{39}\{cis\text{-}Pt(NH_3)_2\}_2]\cdot 11H_2O$ using a similar approach, and demonstrated long-term steady hydrogen production with highly effective utilization of the platinum centers for hydrogen production from aqueous ethylenediamine tetraacetic acid disodium salt (EDTA·2Na) and triethanolamine (TEOA) solutions under visible light irradiation.[11–15]

Furthermore, the utilization of POMs for the stabilization of metal nanoparticles, e.g., silver halides,[16] Ag(0),[17–19] Ir(0),[20–22] Rh(0),[23] Au(0),[24–26] and Pt(0),[27,28] in aqueous and organic solutions because of their high charge has been reported. These colloidal particles are generally obtained by mixing in solutions of metal nanoparticles (or metal species) and POMs and, if necessary, subsequent reduction treatments (by chemical, photochemical, and electrochemical methods) at moderate reaction temperatures; however, the production of colloidal particles of noble metal species and POM composites derived by a simple air-calcination in the solid state has not yet been reported.

In this study, we first derived hydrophilic colloidal nanoparticles composed of platinum hydroxides and a cesium salt of a Keggin-type polyoxotungstate, $Cs_4SiW_{12}O_{40}$, by subjecting a cesium salt of α-Keggin diplatinum(II)-coordinated silicotungstate, $Cs_4[\alpha\text{-}SiW_{11}O_{39}\{cis\text{-}$

Pt^{II}(NH$_3$)$_2$}$_2$]·11H$_2$O (**Cs-Si-Pt**), to direct air calcination at 300 °C in the solid state. By exchanging the four cesium ions with tetramethylammonium ions, colloidal particles composed of platinum hydroxides and tetramethylammonium salts, TMA$_4$SiW$_{12}$O$_{40}$ (here, TMA = [(CH$_3$)$_4$N]$^+$), were also obtained. The obtained particles were characterized by elemental analysis, thermogravimetric/differential thermal analysis (TG/DTA), Fourier transform infrared (FT-IR) spectroscopy, ultraviolet-visible (UV–Vis) spectroscopy, X-ray photoelectron (XPS) spectroscopy, X-ray powder diffraction (PXRD), solution and solid-state ^{29}Si nuclear magnetic resonance (NMR), cold-spray ionization–mass spectrometry (CSI–MS), dynamic light scattering (DLS), zeta potential analysis, and transmission electron microscopy (TEM). The photocatalytic activities of the colloidal particles for hydrogen production from aqueous TEOA solutions in the presence of Eosin Y (EY), Keggin-type mono-aluminum-coordinated polyoxometalates, K$_5$[α-SiW$_{11}${Al(OH$_2$)}O$_{39}$]·7H$_2$O, and titanium dioxide under visible light irradiation (λ = ≥440 nm) were also investigated.

Results and Discussion

Synthesis, characterization, and thermal treatment of a cesium salt of α-Keggin-type diplatinum(II)-coordinated silicotungstate, Cs-Si-Pt

The cesium salt of the α-Keggin-type diplatinum(II)-coordinated silicotungstate, **Cs-Si-Pt**, was synthesized by the 2:1 stoichiometric reaction of *cis*-diamminedichloroplatinum(II) (cisplatin) with mono-lacunary α-Keggin-type polyoxotungstate ([α-SiW$_{11}$O$_{39}$]$^{8-}$) in aqueous solution, followed by the addition of cesium chloride, as previously reported for Cs$_3$[α-PW$_{11}$O$_{39}${*cis*-Pt(NH$_3$)$_2$}$_2$]·8H$_2$O (denoted **Cs-P-Pt**).[11] The purification was carried out by precipitation from water, and **Cs-Si-Pt** was finally isolated as an analytically pure, yellow powder in 66% yield. **Cs-Si-Pt** was characterized by elemental analysis, TG/DTA, FT-IR, solution UV–Vis spectroscopy, and solution ^{1}H NMR and ^{29}Si magic-angle spinning (MAS) NMR spectroscopies (see Experimental), and it was confirmed that the molecular structure was the same as that of [(CH$_3$)$_4$N]$_4$[α-SiW$_{11}$O$_{39}${*cis*-Pt(NH$_3$)$_2$}$_2$]·13H$_2$O (**TMA-Si-Pt**),[14] as shown in Figure 1.
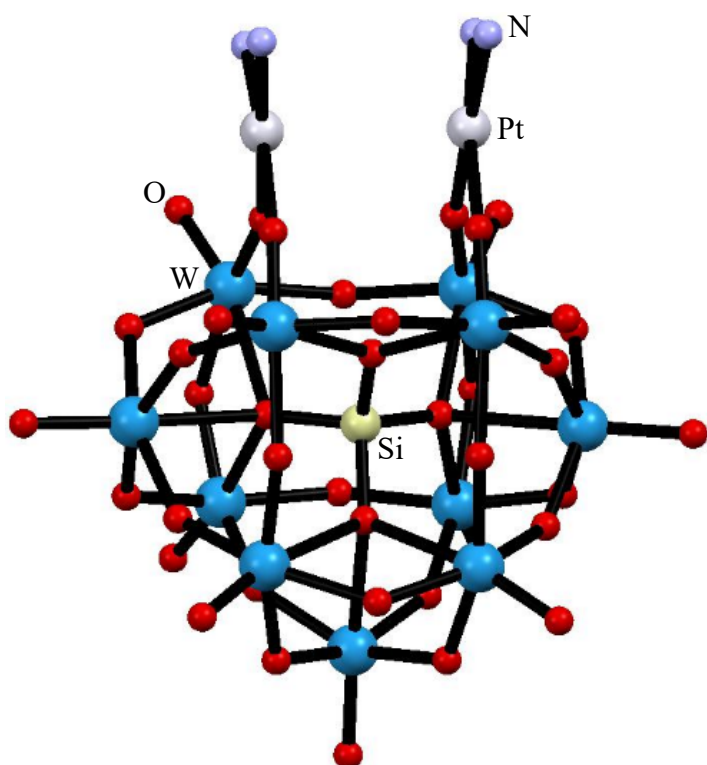
Figure 1. Molecular structure (ball and stick) of $[\alpha\text{-SiW}_{11}\text{O}_{39}\{cis\text{-Pt(NH}_3)_2\}_2]^{4-}$, which crystallized in monoclinic space group $P2_1/n$.[14]

When **Cs-Si-Pt** was calcined at temperatures from ca. 25 to 300 °C at a heating rate of 40 °C min^{-1} followed by holding at 300 °C for 5 h in air (without flow), the color changed from yellow to dark brown (the calcined sample is denoted **Cs-Si-Pt-300-5**, where **Cs-Si-Pt-X-Y** (**X** = calcination temperature (°C); **Y** = calcination time (h)), and the obtained powder was soluble in water. According to the TG/DTA results, the desorption of the four ammonia molecules coordinated to the platinum centers in **Cs-Si-Pt** started at 216.7 °C and was completed at 365.4 °C, as shown in Figure S1. During the thermal treatment at 300 °C for 5 h, the four ammonia molecules in **Cs-Si-Pt** were completely removed, and this was confirmed by nitrogen analysis (<0.1%). The solubility in water was almost unchanged by thermal treatment at 250 and 400 °C for 5 h (the obtained samples are denoted **Cs-Si-Pt-250-5** and **Cs-Si-Pt-400-5**), but a water-insoluble black precipitate was formed when **Cs-Si-Pt** was calcined at 500 °C for 5 h in air (the obtained sample is denoted **Cs-Si-Pt-500-5**).
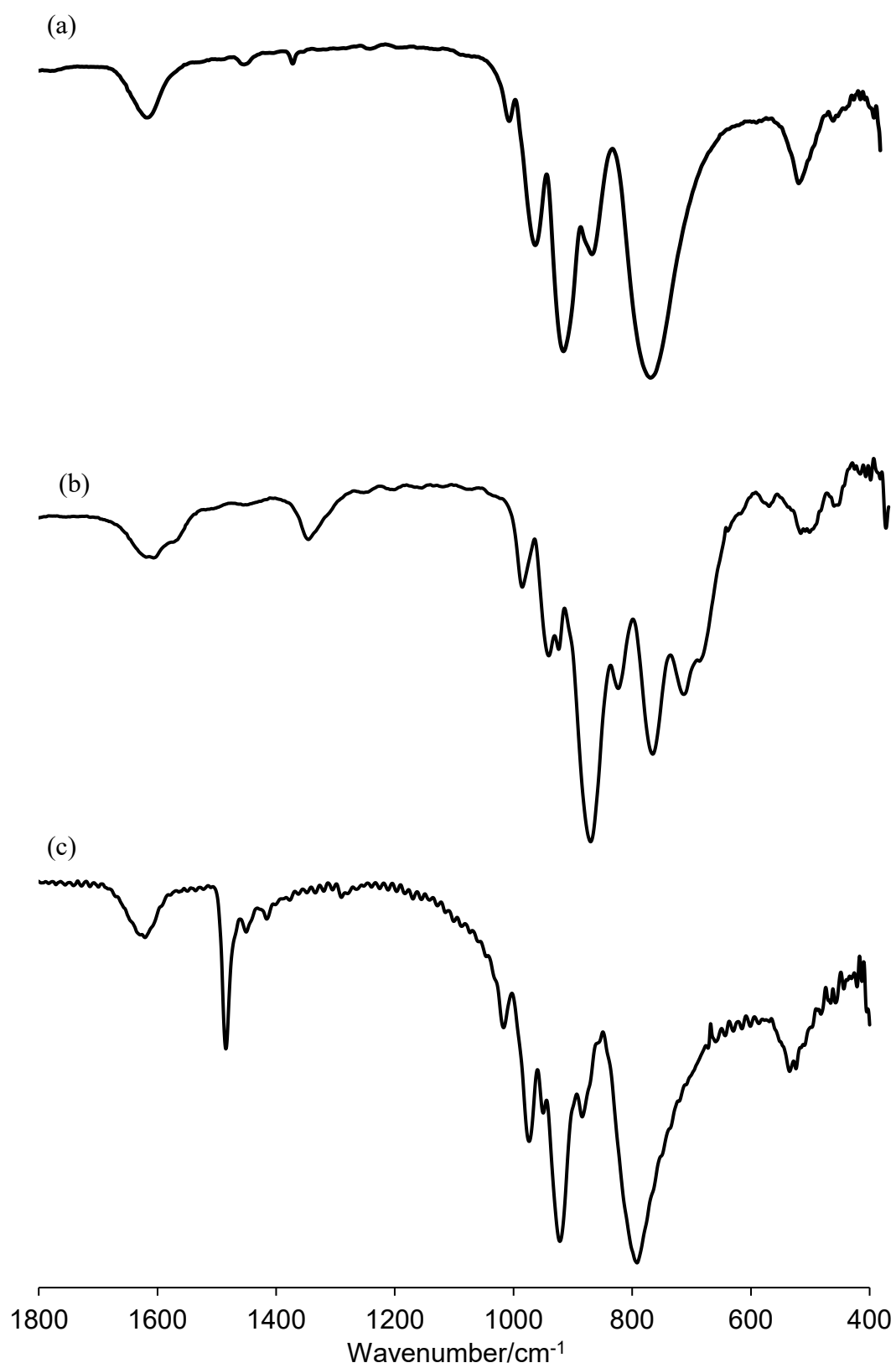
Figure 2. FT-IR spectra (obtained in KBr disks) of (a) **Cs-Si-Pt-300-5**, (b) **Cs-Si-Pt**, and (c) **Cs-Si-Pt-300-5-TMA**.

The FT-IR spectrum (obtained in KBr disk) of **Cs-Si-Pt-300-5** contains several bands at 1017, 974, 927, 882, and 793 cm^{-1} (Figure 2a), which were different from those of **Cs-Si-Pt** (1004, 960, 944, 891, 846, 789, 738, and 712 cm^{-1}) (Figure 2b) and similar to those of $Cs_4SiW_{12}O_{40}$ (1020, 979, 875, and 778 cm^{-1}) [29] and $[Pt(NH_3)_4]_2[\alpha\text{-}SiW_{12}O_{40}]\cdot 4H_2O$ (denoted **Pt-SiW12**) (see Experimental). The spectral pattern of **Cs-Si-Pt-300-5** did not change after reprecipitation from water/ethanol at approximately 25 °C. The same spectra were also obtained for **Cs-Si-Pt-250-5**, **Cs-Si-Pt-400-5**, and **Cs-Si-Pt-500-5**. The band at 1356 cm^{-1}, indicative of the four ammonia groups disappeared, as observed by nitrogen analysis. In the PXRD patterns, no peaks were observed in the 2θ range of 5–90° for **Cs-Si-Pt-250-5**, **-300-5**, and **-400-5**; however, the patterns of **Cs-Si-Pt-500-5** showed some peaks corresponding to $Cs_4SiW_{12}O_{40}$ (Figure S3). This result also supported the formation of $Cs_4SiW_{12}O_{40}$ by the reported thermal treatments.
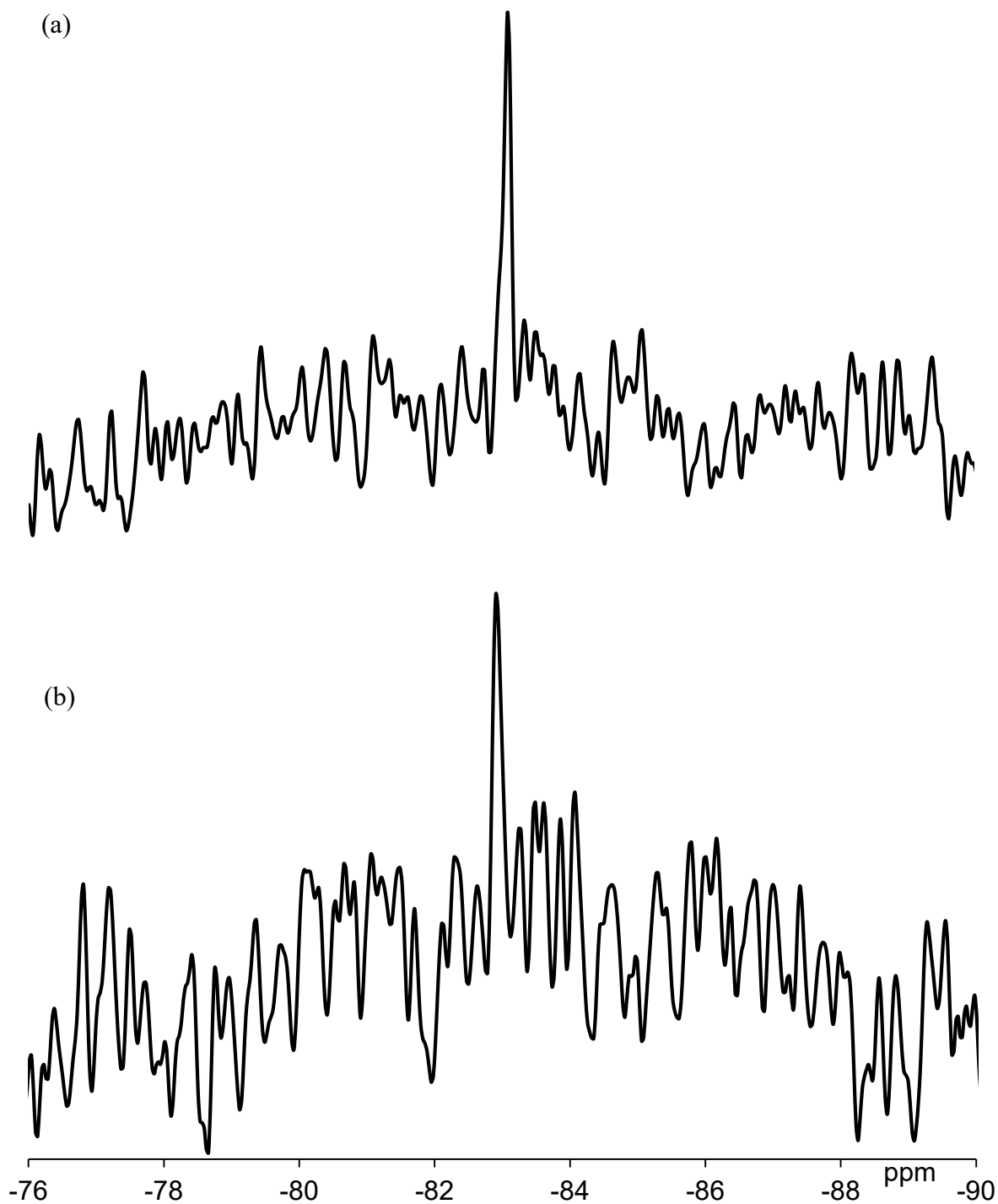
Figure 3. Solution ^{29}Si NMR spectra in D_2O of (a) **Cs-Si-Pt-300-5** and (b) **Cs-Si-Pt-300-5-TMA**.

The solution ^{29}Si NMR spectrum in D_2O of **Cs-Si-Pt-300-5** showed a single-line signal at -83.1 ppm arising from the internal silicon atom, confirming the purity and homogeneity of the

Keggin unit, as shown in Figure 3a. The signal was shifted compared with the signal of α-$SiW_{12}O_{40}^{4-}$ (δ: -84.7) and α-$SiW_{11}O_{39}^{8-}$ (δ: -84.4). Considering the results of the above FT-IR measurements, the α-$SiW_{11}O_{39}^{8-}$ ligand in **Cs-Si-Pt** transferred to α-$SiW_{12}O_{40}^{4-}$, and it interacted with the new platinum species formed by the thermal treatment in the aqueous solution. The ^{29}Si MAS NMR spectrum (Figure 4) of **Cs-Si-Pt-300-5** also contains a signal at -82.5 ppm, and no signal arising from the as-prepared **Cs-Si-Pt** (δ: -85.3) was observed. These results also showed the homogeneity of the calcined sample, even in the solid state.
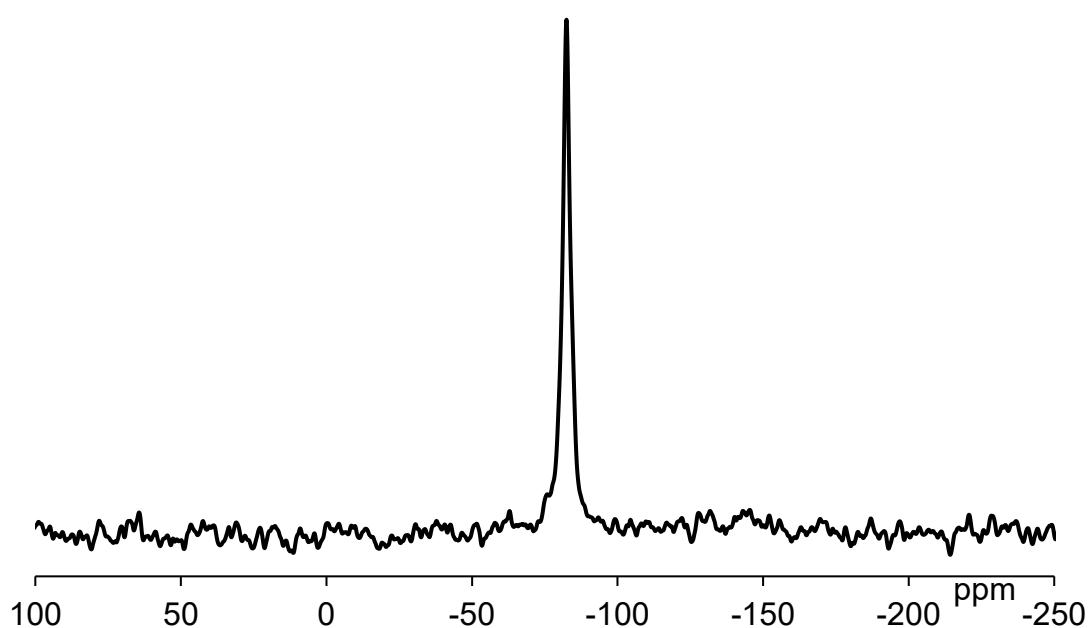

Figure 4. ^{29}Si MAS NMR spectrum of **Cs-Si-Pt-300-5**.

The W(4f) XPS spectra (Figures 5a and 5b) of **Cs-Si-Pt-300-5** and **Cs-Si-Pt** contain peaks at the W($4f_{7/2}$) binding energies of 36.3 and 36.5 eV; this suggests that the tungsten sites in **Cs-Si-Pt-300-5** and **Cs-Si-Pt** were hexavalent (W^{6+}). Moreover, contributions from W^{5+} (around 34.5 eV) and W^{4+} (around 33.5 eV) were not observed.[30–32] Concerning the Pt(4f) XPS spectrum of **Cs-Si-Pt-300-5**, a clear spectrum could not be obtained, and the signals from the Cs(4d) electrons[33] were overlapped in the Pt^{4+} region.[34,35] A clear Pt(4d) XPS spectrum of **Cs-Si-Pt-300-5** not be obtained.

To determine the valence of platinum sites by XPS measurements, we carried out an ion-exchange reaction of cesium ions in **Cs-Si-Pt-300-5** with tetramethylammonium ions, using the

following procedure: **Cs-Si-Pt-300-5** (0.3673 g) was dissolved in water (200 mL) at 25 °C. The solution was filtered through a membrane filter (JG 0.2 μm), and an excess of tetramethylammonium chloride (1.10 g) was added to the solution. After 24 h of stirring at 25 °C, a dark brown precipitate was collected using a membrane filter (JG 0.2 μm). The product was washed with excess ethanol. Yield: 0.1512 g. The obtained powder is denoted **Cs-Si-Pt-300-5-TMA**. The FT-IR spectrum (obtained in a KBr disk) in the polyoxoanion region (1200−600 cm^{-1}) of **Cs-Si-Pt-300-5-TMA** showed bands at 1019, 977, 952, 924, 887, and 796 cm^{-1} (Figure 2c), which are consistent with those of **Cs-Si-Pt-300-5**. The band at 1486 cm^{-1} is due to the tetramethylammonium ions. Since **Cs-Si-Pt-300-5-TMA** has low solubility in water and low stability in solution, it was not possible to obtain a high quality ^{29}Si NMR spectrum in D$_2$O. However, a single-line signal was observed at -82.9 ppm, which is consistent with **Cs-Si-Pt-300-5**, as shown in Figure 3b. No clear signal was observed in the ^{195}Pt NMR spectrum of **Cs-Si-Pt-300-5-TMA**, as reported for Pt^{2+}-containing POMs.[12,36] The W(4f) XPS spectrum of **Cs-Si-Pt-300-5-TMA** also contains the W(4f$_{7/2}$) binding energy at 36.3 eV, as shown in Figure 5c. This result indicates that the tungsten sites were in the hexavalent charge state, W^{6+}, after the ion-exchange reaction, and contributions from W^{4+} and W^{5+} were not observed. The Pt(4f) XPS spectrum was quite noisy, as shown in Figure 6a. However, a Pt(4f$_{7/2}$) peak was observed at a binding energy of 73.8 eV, which is consistent with Pt^{2+} in cisplatin (73.5 eV; Figure 6b), and no contribution from Pt^0 (around 71 eV) was observed.[32,35] For K$_2$[Pt^{IV}Cl$_6$], the Pt(4f$_{7/2}$) binding energy at 76.4 eV was assigned to Pt^{4+}, as shown in Figure 6c. Thus, the oxidation state of the platinum sites in **Cs-Si-Pt-300-5** and **Cs-Si-Pt-300-5-TMA** was Pt^{2+}. This result suggests that the [*cis*-Pt(NH$_3$)$_2$]$^{2+}$ moieties were oxidized (e.g., transformed to PtO and Pt(OH)$_2$) by the thermal treatment.
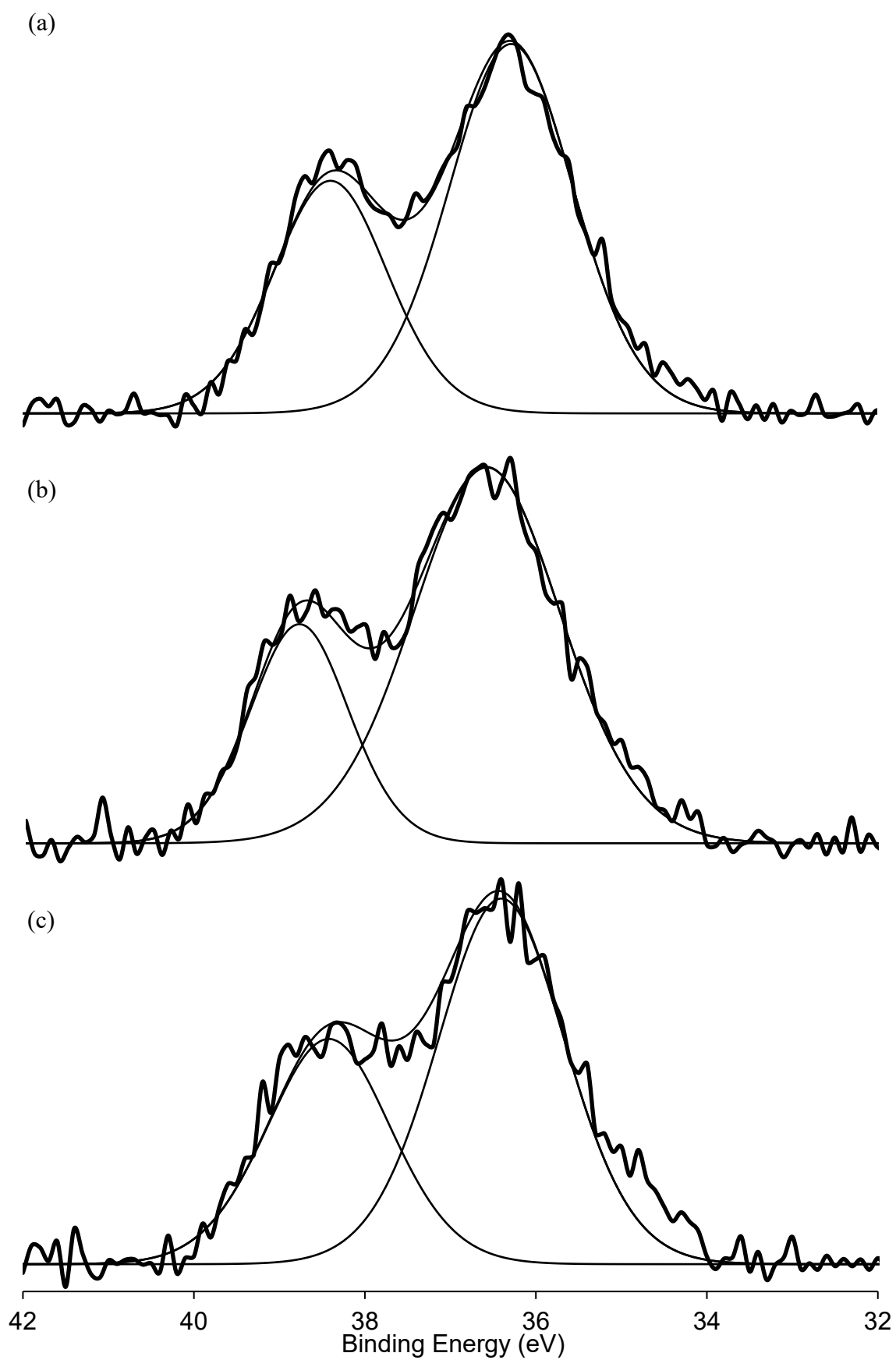
Figure 5. W(4f) XPS spectra of (a) **Cs-Si-Pt-300-5**, (b) **Cs-Si-Pt**, and (c) **Cs-Si-Pt-300-5-TMA**.
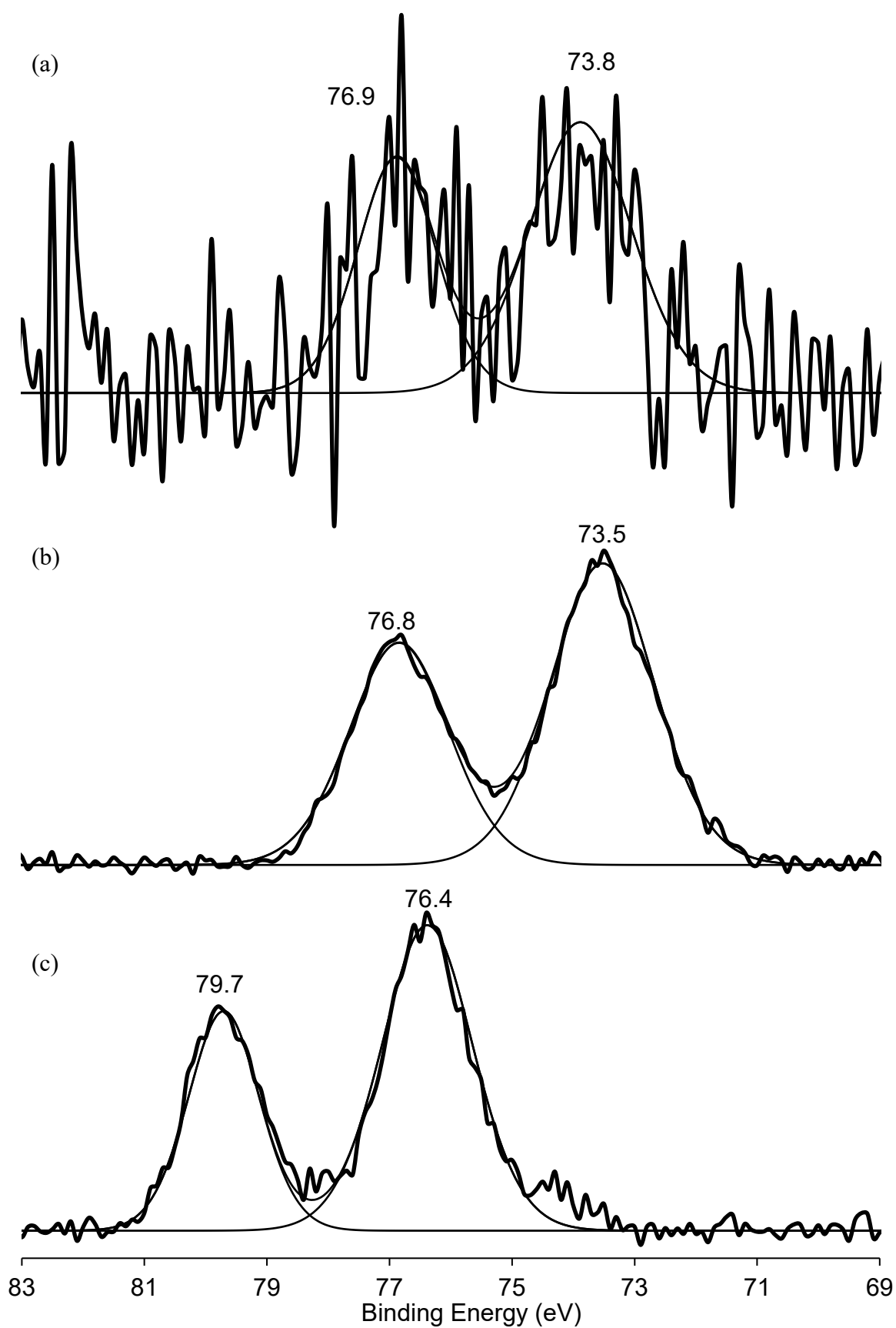
11

Figure 6. Pt(4f) XPS spectra of (a) **Cs-Si-Pt-300-5-TMA**, (b) cisplatin, and (c) $K_2[Pt^{IV}Cl_6]$.

The elemental analysis of **Cs-Si-Pt-300-5-TMA** afforded the following results: hydrogen, 1.4%; carbon, 5.3%; nitrogen, 1.5%; silicon, 0.92%; platinum, 11.2%; and cesium, < 0.1%. Because the divalent platinum site retained a planar four-coordinate structure,[37,38] it was presumed that **Cs-Si-Pt-300-5-TMA** had a structure in which the $Pt(OH)_2$ species coordinated with the surface of $SiW_{12}O_{40}^{4-}$. The results are consistent with the values calculated from the following formula, $[(CH_3)_4N]_4[\{Pt(OH)_2\}_2 \cdot SiW_{12}O_{40}]$: hydrogen, 1.44%; carbon, 5.30%; nitrogen, 1.54%; silicon, 0.77%; platinum, 10.75%; and cesium, 0%. The four cesium ions in **Cs-Si-Pt-300-5** were completely exchanged by four tetramethylammonium ions; however, the two platinum atoms were not removed by the ion-exchange reaction. This indicates that the two platinum atoms interacted with the surface of $SiW_{12}O_{40}^{4-}$ (not as countercations). Figure 7 shows the CSI–MS spectrum obtained in a water/acetonitrile (1/1 (v/v)) solution of **Cs-Si-Pt-300-5-TMA**. The spectrum exhibits peaks at $m/z = 1511.1$ and 3096.1, which are assigned to $[TMA_2(SiW_{12}O_{40})]^{2-}$ (*m/z* 1511.2) and $[TMA_3(SiW_{12}O_{40})]^-$ (*m/z* 3096.5), respectively. This also indicates that the $\{SiW_{11}O_{39}\}$ ligand in **Cs-Si-Pt** was transformed to $\{SiW_{12}O_{40}\}$ under the reported thermal treatment conditions. Thus, **Cs-Si-Pt-300-5** also contains $Cs_4[\{Pt(OH)_2\}_2 \cdot SiW_{12}O_{40}]$.

The formation of hydrophilic colloidal particles of **Cs-Si-Pt-300-5** in a saturated aqueous solution at different pH values of 4.1, 5.0, 6.0, and 7.2, was monitored by the DLS technique, as shown in Figure 8. At each pH value, the colloid particles had a particle size distribution in the range of 80–285 nm, and particles with a size of 6500 nm or more were also observed. The zeta potential values were ⁻47.99, ⁻49.74, ⁻49.90, and ⁻53.31 mV, suggesting that the hydrophilic colloid particles were formed by the aggregation of the anionic POM, $[\{Pt(OH)_2\}_2 \cdot SiW_{12}O_{40}]^{4-}$, in aqueous solution.[39,40] The TEM image of **Cs-Si-Pt-300-5-TMA** produced from the aqueous solution shows particle aggregates consisting of **Cs-Si-Pt-300-5-TMA** (Figure S4a). The TEM images of **Cs-Si-Pt-300-5-TMA** and **Cs-Si-Pt-300-5** shown in Figures S4b and S5 show that larger particles are formed in solution. These results supported the result that $[\{Pt(OH)_2\}_2 \cdot SiW_{12}O_{40}]^{4-}$ aggregated to form a supramolecular structure.
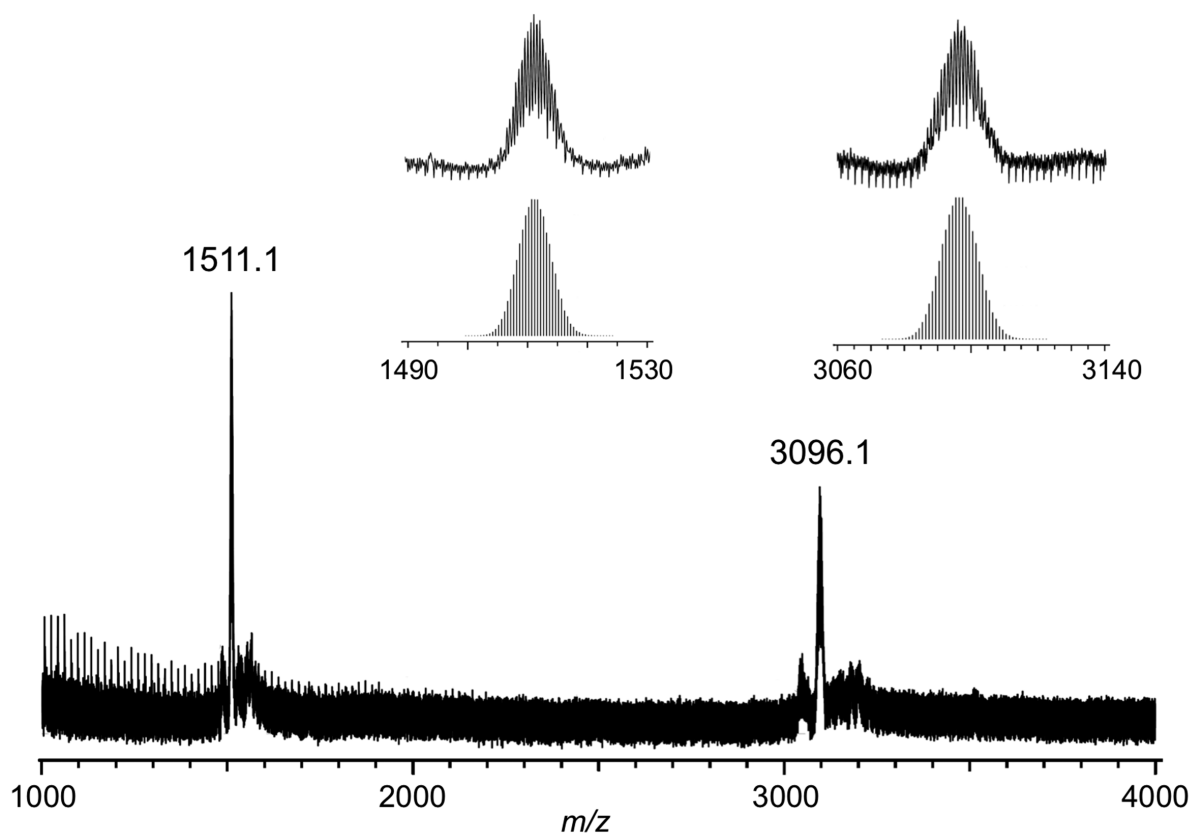
Figure 7. CSI-MS spectrum of **Cs-Si-Pt-300-5-TMA** in acetonitrile/water (1/1 v/v). Inset: spectra in the *m/z* range of 1490–1530 and 3060–3140, and the calculated patterns for $[TMA_2(SiW_{12}O_{40})]^{2-}$ (*m/z* 1511.2) and $[TMA_3(SiW_{12}O_{40})]^-$ (*m/z* 3096.5).
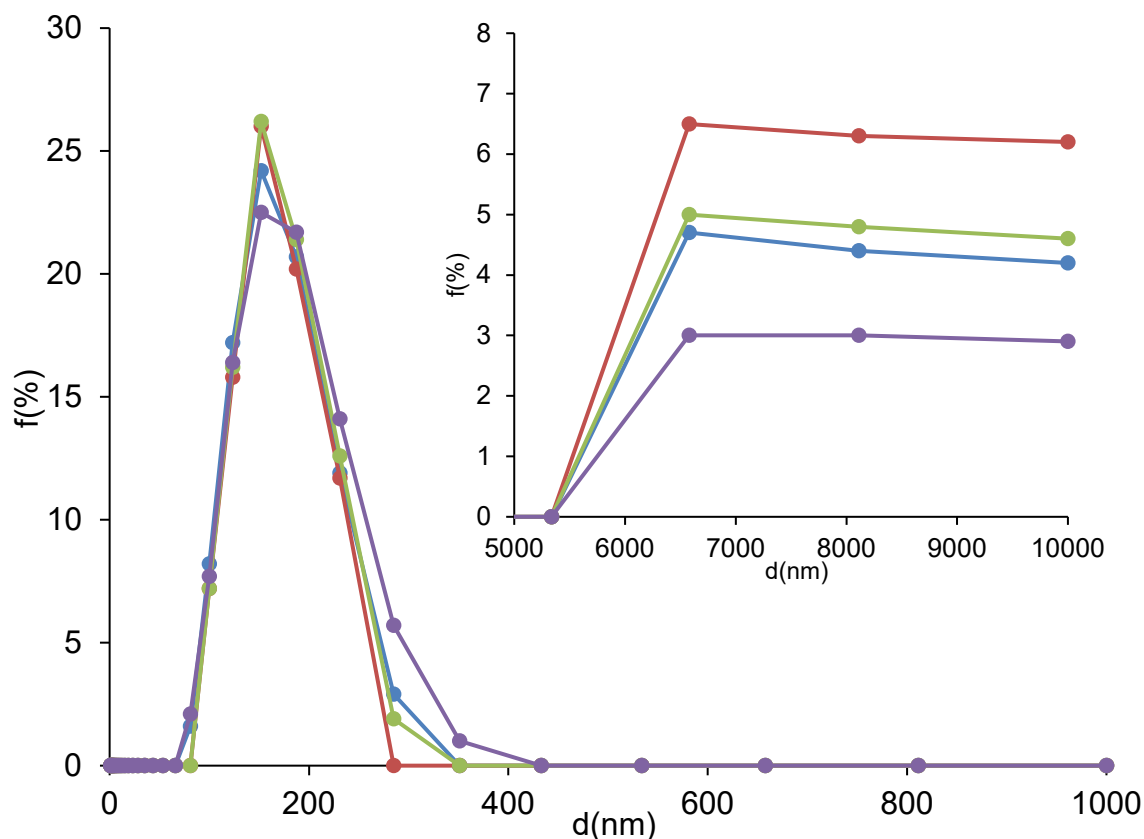
Figure 8. Colloidal particle size distribution of **Cs-Si-Pt-300-5** in the saturated solution, as monitored by DLS. The measurements were carried out at pH values of 4.1 (blue), 5.0 (red), 6.0 (green), and 7.2 (purple).

The UV–Vis spectra of **Cs-Si-Pt-300-5** and **Cs-Si-Pt-300-5-TMA** in aqueous solution are shown in Figure 9. The spectrum of the as-prepared **Cs-Si-Pt** contains absorption bands at 245 nm and approximately 325 and 409 nm from 220 to 800 nm (Figure S2). The bands at 245 and at around 325 nm were assigned to the charge transfer (CT) band of W^{6+}-O and a broad band at around 409 nm was assigned to the two platinum(II) atoms, as previously reported for $Cs_3[\alpha$-$PW_{11}O_{39}\{cis$-$Pt(NH_3)_2\}_2]\cdot 8H_2O$.[11] For **Cs-Si-Pt-300-5** and **Cs-Si-Pt-300-5-TMA**, a CT band of W^{6+}-O was observed at 260 and 265 nm, respectively. These were shifted from that of **Cs-Si-Pt** and were similar to that of α-$SiW_{12}O_{40}^{4-}$ (at 263 nm). This also supports the hypothesis that the $\{SiW_{11}O_{39}\}$ ligand in **Cs-Si-Pt** was transformed to $\{SiW_{12}O_{40}\}$ under the reported thermal treatment conditions. A clear band was not observed in the range of 300 – 800 nm; however, it was noticed that the absorption shifted toward longer wavelengths than that observed for **Cs-Si-Pt**. Because α-$SiW_{12}O_{40}^{4-}$ does not absorb light in the visible region, it can be inferred that the change in the absorption band in the visible region is due to the formation

15

of colloidal particles containing platinum hydroxide species in solution.
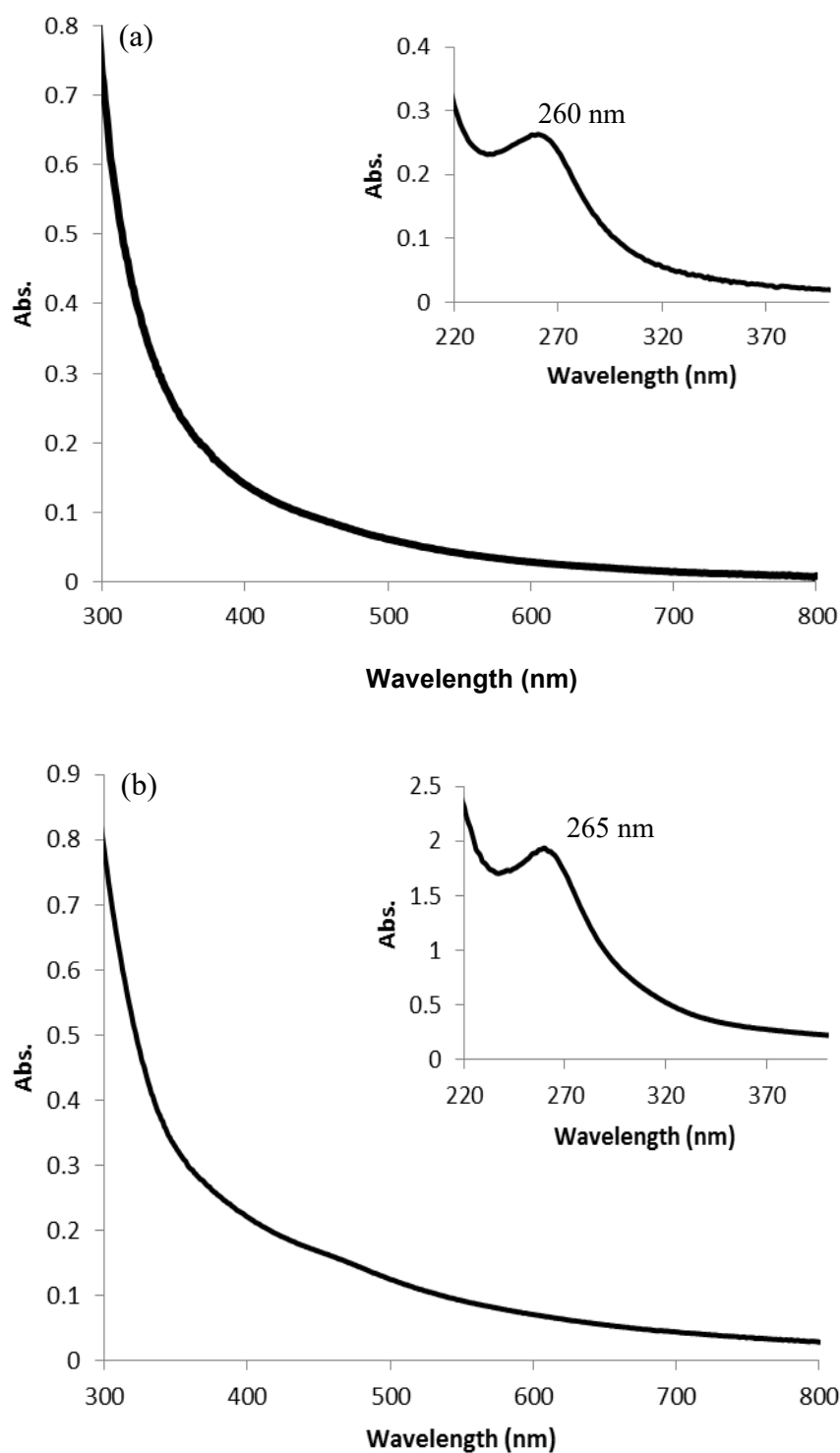

Figure 9. Solution UV-Vis spectra in water of (a) **Cs-Si-Pt-300-5** and (b) **Cs-Si-Pt-300-5-TMA** in the range of 300–800 nm. In (b), the concentration of **Cs-Si-Pt-300-5-TMA** is 4.7 × 10^{-5} M. Inset: in the range of 220–400 nm. In the inset of (b), the concentration of **Cs-Si-Pt-300-5-TMA** is 4.6 × 10^{-6} M.

When **Cs-P-Pt** or **Pt-SiW12** was calcined at 300 °C for 5 h, an insoluble black solid was formed. When cisplatin was heat-treated under the same conditions, a reduction to platinum (0) occurred. The formation of several intermediate has been reported during air-calcining treatment of platinum compounds such as H_2PtCl_6, $Pt(NH_3)_4Cl_2$, $Pt(NH_3)_4(OH)_2$, $Pt(NH_3)_4(NO_3)_2$, $H_2Pt(OH)_6$, and $Pt(C_5H_7O_2)_2$; however, their isolation as solids has not been reported.[41]

Photocatalytic activities of the calcined samples for hydrogen evolution from an aqueous TEOA under visible light irradiation

As a technique for improving the utilization efficiency of platinum atoms for the production of hydrogen from water under light irradiation, co-catalyst modification (such as size control of platinum nanoparticles [42–44] and alloying [45,46]) have been developed. Although they exhibit efficient photocatalytic activities, it still be difficult to control the platinum nanostructures by the thermal decomposition or photolysis of platinum compounds (such as H_2PtCl_6 and $Pt(NH_3)_4(NO_3)_2$). There are also reports of platinum(II)-based hydrogen-evolving catalysts; however, platinum utilization efficiency is not so high under the reported conditions.[47,48]

To investigate the activities of the isolated platinum(II) sites constructed in the **Cs-Si-Pt-300-5** as a co-catalyst, we demonstrated the hydrogen evolution in aqueous TEOA in the presence of **Cs-Si-Pt-300-5**, EY, $K_5[\alpha\text{-}SiW_{11}\{Al(OH_2)\}O_{39}]\cdot7H_2O$ (denoted **K-Si-Al**), and titanium dioxide (anatase:rutile = 80:20) under light irradiation ($\lambda = \geq440$ nm), as shown in Figure 10a. **Cs-Si-Pt-300-5** was obtained by weighing **Cs-Si-Pt** while ensuring that the amount of platinum was 0.2 μmol; subsequently, it was calcined at 300 °C for 5 h in air. TEOA was used as the sacrificial reagent.[13,49] **Cs-Si-Pt-300-5**, EY, and **K-Si-Al** were used as co-catalyst, photosensitizer, and EY stabilizer, respectively.[13,49] TiO_2 was used to promote charge separation.[50] Hydrogen was formed with 100% selectivity, and oxygen, carbon dioxide, carbon monoxide, and methane were not detected under these reaction conditions. As control experiments, no reaction was observed in the absence of platinum catalysts or Eosin Y under the reported conditions.
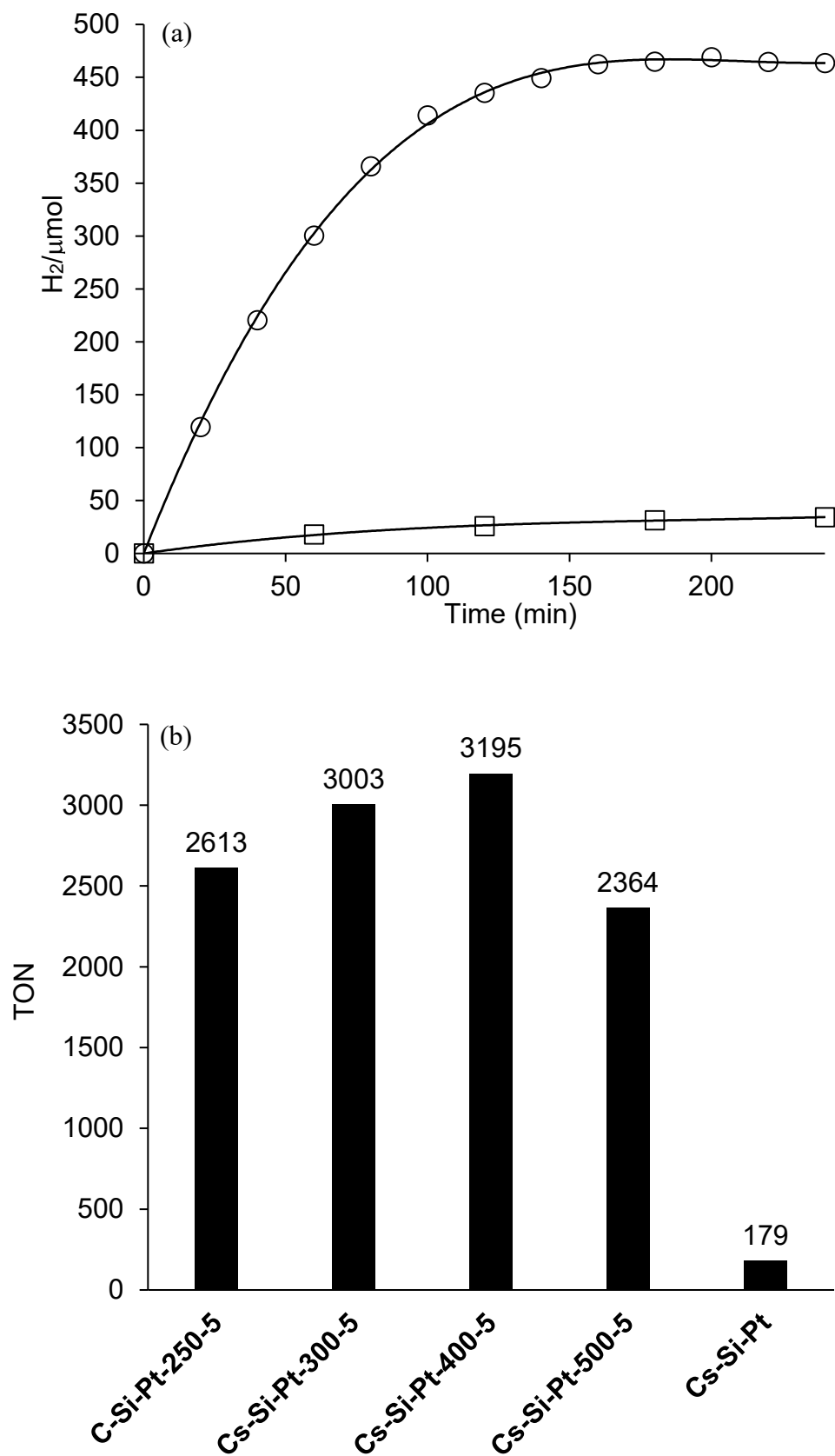
Figure 10. (a) Time course for hydrogen evolution from aqueous TEOA under visible light irradiation. (b) TON after 1 h of irradiation for hydrogen evolution from aqueous TEOA under

visible light irradiation catalyzed by **Cs-Si-Pt-250-5**, **Cs-Si-Pt-300-5**, **Cs-Si-Pt-400-5**, **Cs-Si-Pt-500-5**, and **Cs-Si-Pt**. Reaction conditions: **Cs-Si-Pt-300-5** (○) and **Cs-Si-Pt** (□) (0.2 μmol Pt), EY (2.5 μmol), **K-Si-Al** (2.5 μmol), TiO_2 (anatase:rutile = 80:20) 50 mg, 100 mM TEOA aqueous solution (10 mL, pH 7), light irradiation ($\lambda = \geq 440$ nm), 25 °C.

After 1 h of light irradiation, **Cs-Si-Pt-300-5** (0.2 μmol of Pt) evolved 300.3 μmol of hydrogen, and the TON (= 2[hydrogen evolved (mol)]/[Pt atoms (mol)]) reached 3003. The activities were approximately 17 times higher than that of **Cs-Si-Pt** (the amount of hydrogen evolved after 1 h was 17.9 μmol; TON, 179) under the same reaction conditions. The activity after 1 h was similar to that of **Cs-Si-Pt-300-5-TMA** (the amount of hydrogen evolved was 358.9 μmol; TON, 3589); this also supported the result that the composition of $[\{Pt(OH)_2\}_2 \cdot SiW_{12}O_{40}]^{4-}$ in **Cs-Si-Pt-300-5** was not changed by the ion-exchange reaction of cesium ions with tetramethylammonium ions. Relatively rapid deactivation was observed for 2 h; however, the TON exceeded 4600 after 3 h of light irradiation. The turnover frequency (TOF = TON/reaction time (h)) of **Cs-Si-Pt-300-5** was 3588 h^{-1} after 20 min, which was higher than those of similar photocatalytic systems containing platinum co-catalyst prepared by photoreduction of H_2PtCl_6, EY, and TiO_2. For example, the TOFs of Pt/EY/nitrogen-doped TiO_2,[51] Pt/EY/modified TiO_2 with phosphate,[52] and EY/Pt/$SiW_{11}O_{39}^{8-}$/TiO_2[50] are less than 100 h^{-1} for hydrogen evolution from aqueous TEOA solutions under visible-light irradiation. **Cs-Si-Pt-400-5** had the same TON as **Cs-Si-Pt-300-5**. **Cs-Si-Pt-250-5** and **Cs-Si-Pt-500-5** had higher TONs than **Cs-Si-Pt**, as shown in Figure 10b. These results indicated that the thermal treatment significantly improved the photocatalytic activities of **Cs-Si-Pt**, and, in particular, it was found that the catalysts obtained by calcining **Cs-Si-Pt** at 300 and 400 °C for 5 h exhibited high catalytic activities under the reported reaction conditions.

A probable reaction mechanism for the **Cs-Si-Pt-300-5**/EY/**K-Al-1**/TiO_2 system is as follows:[13,50] EY absorbs photon energy to produce excited EY* in the initial step and, subsequently, injects electrons into the conduction band of TiO_2 or the tungsten sites in **Cs-Si-Pt-300-5** and **K-Si-Al** to form a reduced species (heteropoly blue species). The electrons injected into the conduction band of TiO_2 are consumed by the reduction of water at the platinum sites in **Cs-Si-Pt-300-5** to form hydrogen. When Keggin-type diplatinum(II)-coordinated polyoxotungstates are used as a photocatalyst, the heteropoly blue species act as photosensitizers to achieve long-term hydrogen production. However, relatively rapid

deactivation was observed for **Cs-Si-Pt-300-5**, and the activity did not improve even when EY was added again. This could be due to the decomposition of **Cs-Si-Pt-300-5** under the reported reaction conditions. Investigations into the stabilization of $[\{Pt(OH)_2\}_2 \cdot SiW_{12}O_{40}]^{4-}$ is in progress.

Conclusions

Hydrophilic platinum-polyoxotungstate colloidal particles formed by the self-assembly of $Cs_4[\{Pt(OH)_2\}_2 \cdot SiW_{12}O_{40}]$ were obtained by the calcination of an α-Keggin-type diplatinum(II)-coordinated silicotungstate, $Cs_4[\alpha-SiW_{11}O_{39}\{cis-Pt(NH_3)_2\}_2] \cdot 11H_2O$ (**Cs-Si-Pt**), in air at 300 °C for 5 h. The ion-exchange reaction of **Cs-Si-Pt-300-5** with tetramethylammonium ions afforded a tetramethylammonium salt, $[(CH_3)_4N]_4[\{Pt(OH)_2\}_2 \cdot SiW_{12}O_{40}]$, which also formed hydrophilic colloidal particles in aqueous solution. The calcined sample acted as a photocatalyst for hydrogen evolution from aqueous TEOA solution under visible light irradiation ($\lambda = \geq440$ nm) in the presence of EY, $K_5[\alpha-SiW_{11}\{Al(OH_2)\}O_{39}] \cdot 7H_2O$, and titanium dioxide. Although relatively rapid deactivation was observed for 2 h, it was surprising that the TOF achieved was 3588 h^{-1} after 20 min, and the TON exceeded 4600 after 3 h of light irradiation. Thus, $[\{Pt(OH)_2\}_2 \cdot SiW_{12}O_{40}]^{4-}$ is the first isolated platinum intermediate formed by the thermal treatment of a platinum complex as a solid. Our results also demonstrate that the photocatalytic activity of platinum as a co-catalyst was significantly improved by the thermal treatment of α-Keggin-type diplatinum(II)-coordinated silicotungstate under the reported conditions.

Experimental Section

Materials: $K_4[\alpha-SiW_{12}O_{40}] \cdot 17H_2O$,[53] $K_8[\alpha-SiW_{11}O_{39}] \cdot 17H_2O$,[54] $Cs_3[\alpha-PW_{11}O_{39}\{cis-Pt(NH_3)_2\}_2] \cdot 8H_2O$ (denoted as **Cs-P-Pt**),[11] and $K_5[\alpha-SiW_{11}\{Al(OH_2)\}O_{39}] \cdot 7H_2O$[55] were prepared as described in the literature. The number of solvated water molecules was determined by TG/DTA. $[Pt(NH_3)_4]_2[\alpha-SiW_{12}O_{40}] \cdot 4H_2O$ (denoted **Pt-SiW12**) was prepared as follows: $[Pt(NH_3)_4]Cl_2$ (0.4 mmol) was dissolved in water (150 mL) and added to an aqueous solution (50 mL) of $K_4[\alpha-SiW_{12}O_{40}] \cdot 17H_2O$ (0.2 mmol) at 25 °C. After stirring for 1 h at 25 °C, the white–yellow precipitate was collected using a membrane filter (JG 0.2 μm), and washed with

water (50 mL × 5). The numbers of $[Pt(NH_3)_4]^{2+}$ countercations and solvated water molecules were determined by nitrogen, hydrogen, silicon, and platinum analyses. Found: N, 3.13%; H, 0.92%; Si, 0.81%; Pt, 10.9%. Calcd: N, 3.23%; H, 0.93%; Si, 0.81%; Pt, 11.2% for $[Pt(NH_3)_4]_2[\alpha\text{-}SiW_{12}O_{40}]\cdot4H_2O$. FT-IR (KBr disk): 1341 (NH_3), 1016, 973, 925, 883, 788 cm^{-1}. All the reagents and solvents were obtained from commercial sources and were used as received. Titanium dioxide (anatase:rutile = 80:20) was obtained from Wako Pure Chemical Industries, Ltd. (Japan).

Instrumentation/analytical procedures: Elemental analyses were performed using a Flash EA (Thermo Electron Corporation) and an Optima 2100DV (PerkinElmer Inc.) at Shizuoka University or by sending samples to the Mikroanalytisches Labor Pascher (Remagen, Germany). The TG/DTA data were obtained using a Rigaku Thermo Plus EVO2 TG/DTA 81205Z instrument. Measurements were carried out in air by increasing the temperature from 20 to 500 °C at a rate of 4 °C/min. The IR spectra were recorded on a PerkinElmer Spectrum100 FT-IR spectrometer in KBr disks at approximately 25 °C in air. The ^{1}H (600.17 MHz) and ^{29}Si (119.23 MHz) NMR spectra in solutions were recorded in 5-mm outer diameter tubes on a JEOL ECA-600 NMR spectrometer. The ^{1}H NMR spectra were measured in DMSO-d_6 with respect to an internal standard (the sodium salt of 3-(trimethylsilyl)-1-propanesulfonic acid (DSS)). Chemical shifts are reported as positive for resonances downfield of DSS (δ: 0). The ^{29}Si NMR spectra were measured in D_2O with respect to an external tetramethylsilane (TMS) standard. Chemical shifts are reported as negative on the δ scale for resonances upfield of TMS (δ: 0). The ^{29}Si MAS NMR spectra were recorded at 400 MHz on a JEOL JNM-ECA 400 FT-NMR spectrometer with a JEOL ECP-400 NMR data-processing system. ^{29}Si MAS NMR chemical shifts are reported as negative relative to polydimethylsilane (δ: −34.0). The solution UV–Vis spectra were recorded using a PerkinElmer Spectrum Lambda 650 spectrophotometer. XPS was carried out using an ESCA3400 (Shimadzu Corp., Japan) spectrometer using a non-monochromatic Mg $K\alpha$ radiation source (1253.6 eV). The binding energies are referenced to the C_{1s} binding energy at 284.6 eV for convenience. Powder XRD measurements were performed using an X-ray powder diffractometer (SmartLab, Rigaku, Corp., Japan) using Cu $K\alpha$ radiation (λ = 1.54 Å). TEM images were obtained using a JEM-1400 instrument (JEOL, Tokyo, Japan). The calcined samples were dissolved in water (0.25 mg/L for **Cs-Si-Pt-300-5** and 1 mg/mL for **Cs-Si-Pt-300-5-TMA**), and the solutions were dropped on a hydrophilized

grid and air-dried. The negative-ion CSI–MS spectra were recorded on JEOL JMS-T100CS (acetonitrile/water = 1/1, 0.25 mg/mL; spray temperature, 0 °C) at the University of Tokyo. DLS and zeta potential measurements were performed by Otsuka Electronics Co., Ltd., Japan using an ELSZ-2000 instrument. For the measurements, the calcined sample was dissolved in water (less than 0.5 g/100 mL). The pH values of the solutions were 4.1, 5.0, 6.0, and 7.2. The pH was adjusted by adding aqueous 0.01 M NaOH solution.

Synthesis of Cs-Si-Pt: $K_8[SiW_{11}O_{39}] \cdot 14H_2O$ (0.648 g; 0.20 mmol) and *cis*-$Pt(NH_3)_2Cl_2$ (0.120 g; 0.40 mmol) were dissolved in 200 mL of water at 25 °C. After stirring for 3 h at approximately 90 °C, the solution was filtered through a membrane filter (JG 0.2 μm). CsCl (1.52 g; 9.0 mmol) was added to the filtrate, followed by stirring overnight at 25 °C. Thereafter, a yellow precipitate was collected using a membrane filter (JG 0.2 μm) and washed with a small amount of ethanol. For purification, the obtained product was dissolved in water (6 mL of water per 100 mg of product) at 70 °C. After standing overnight at 25 °C, a yellow precipitate was obtained. The obtained product weighed 0.5062 g (the yield, based on [mol of **Cs-Si-Pt**]/[mol of $K_8[SiW_{11}O_{39}] \cdot 14H_2O] \times 100$, was 66%). Elemental analysis afforded the following results: hydrogen, 0.61%; nitrogen, 1.45%; silicon, 0.70%; tungsten, 52.1%; platinum, 10.3%; cesium, 13.4%. The calculations for $Cs_4[SiW_{11}O_{39}\{cis\text{-}Pt(NH_3)_2\}_2] \cdot xH_2O$ (x = 11) = $H_{34}Cs_4Si_1N_4O_{50}Pt_2W_{11}$: H, 0.89; N, 1.45; Si, 0.73; W, 52.36; Pt, 10.10; Cs, 13.76%. TG/DTA, under atmospheric conditions showed a weight loss of 4.15% with endothermic peaks observed below 210.2 °C at temperatures of 82.1 °C and 94.5 °C, and the calculations indicated a 5.13% loss corresponding to 11 water molecules (Figure S1). Additionally, a weight loss of 1.41% with an exothermic peak at 335.9 °C was observed between 216.7 and 365.4 °C; the calculations indicated four ammonia molecules (calcd: 1.76%). IR (KBr disk) results in the $1300 – 400$ cm^{-1} region (polyoxometalate region) (Figure 2b) showed bands at 1004, 960, 944, 891, 846, 789, 738, and 712 cm^{-1}. ^{1}H NMR (DMSO-*d_6*, 19.4 °C): 4.20 (NH$_3$) and 4.40 (NH$_3$). ^{29}Si MAS NMR: δ: -85.30. UV–vis absorption (in H$_2$O, 4.9×10^{-5} M and 6.8×10^{-6} M) (Figure S2) showed a band at 245 nm (ε 45000 M^{-1} cm^{-1}) and broad bands at around 325 nm (ε 6447 M^{-1} cm^{-1}) and 409 nm (ε 1010 M^{-1}cm^{-1}).

Thermal treatment conditions: The thermal treatments of the platinum compounds were

performed using a muffle furnace (FO100; Yamato Scientific Co., Ltd., Japan). The platinum compounds were typically calcined at temperatures from 25 to 300 °C at a heating rate of 40 °C min^{-1}, followed by holding at 300 °C for 5 h in air (without flow).

Photocatalytic reaction experiments: Typical photocatalytic reactions were carried out at 25 °C. The platinum compounds (0.2 μmol Pt), EY (2.5 μmol), and $K_5[\alpha$-$SiW_{11}\{Al(OH_2)\}O_{39}]\cdot 7H_2O$ (2.5 μmol) were dissolved in 10 mL of 100 mM aqueous TEOA solution at pH 7.0. Subsequently, titanium dioxide (anatase:rutile = 80:20; 50 mg) was added to the aqueous solution. The reaction suspension was put into a glass reaction vessel that, was connected to a Pyrex conventional closed gas circulation system (245.5 cm^3). The photoreaction was initiated by light irradiation using a 300 W Xe lamp equipped with a cut-off filter ($\lambda = \geq 440$ nm). Hydrogen, oxygen, carbon monoxide, and methane evolutions were analyzed by gas chromatography (GC) (with thermal conductivity detector (TCD), 5 Å molecular sieves, and stainless-steel columns). The samples were assigned after comparing them with standard samples analyzed under the same conditions. The turnover number (TON) was calculated as 2[H_2 evolved (mol)]/[Pt atoms (mol)].

Acknowledgments

References

[1] J. Willkomm, K. L. Orchard, A. Reynal, E. Pastor, J. R. Durrant, E. Reisner, *Chem. Soc. Rev.* **2016**, 45, 9–23.

[2] K. C. Christoforidis, P. Fornasiero, *ChemCatChem* **2017**, *9*, 1523–1544.

[3] R. Abe, *J. Photochem. Photobiol. C: Photochem. Rev.* **2010**, *11*, 179–209.

[4] J. Yang, D. Wang, H. Han, C. Li, *Acc. Chem. Res.* **2013**, *46*, 1900–1909.

[5] M. T. Pope, *Heteropoly and Isopoly Oxometalates*, Springer-Verlag, Berlin; New York, **1983**.

[6] M. T. Pope, A. Müller, *Angew. Chem.* **1991**, *103*, 56–70; *Angew. Chem., Int. Ed. Engl.* **1991**, *30*, 34–48.

[7] M. T. Pope and A. Müller, *Polyoxometalates: From Platonic Solids to Anti-Retroviral Activity*, Springer Netherlands, **1994**.

[8] T. Yamase, M.T. Pope, *Polyoxometalate Chemistry for Nano-Composite Design*, Springer US, **2006**.

[9] M. N. Sokolov, S. A. Adonin, E. V. Peresypkina, V. P. Fedin, *Dalton Trans.* **2012**, *41*, 11978–11979.

[10] Z. Lin, N. V. Izarova, A. Kondinski, X. Xing, A. Haider, L, Fan, N. Vankova, T. Heine, B. Keita, J. Cao, C. Hu, U. Kortz, *Chem. Eur. J.* **2016**, *22*, 5514–5519.

[11] C. N. Kato, Y. Morii, S. Hattori, R. Nakayama, Y. Makino, H. Uno, *Dalton Trans.* **2012**, *41*, 10021–10027.

[12] M. Kato, C. N. Kato, *Inorg. Chem. Commun.* **2011**, *14*, 982–985.

[13] S. Hattori, Y. Ihara, C.N. Kato, *Catal. Letters* **2015**, *145*, 1703–1709.

[14] C. N. Kato, S. Suzuki, Y. Ihara, K. Aono, R. Yamashita, K. Kikuchi, T. Okamoto, H. Uno, *Modern Res. Catal*. **2016**, *5*, 103–129.

[15] C. N. Kato, S. Suzuki, T. Mizuno, Y. Ihara, A. Kurihara, S. Nagatani, *Catal. Today*, **2019**, *332*, 2–10.

[16] E. Matijević, K. G. Mathai, M. Kerker, *J. Phys. Chem.* **1963**, *67*, 1995–1999.

[17] O. Siiman, H. Feilchenfeld, *J. Phys. Chem.* **1988**, 92, 453–464.

[18] A. Neyman, L. Meshi, L. Zeiri, I. A. Weinstock, *J. Am. Chem. Soc.* **2008**, *130*, 16480–16481.

[19] C. Costa-Coquelard, D. Schaming, I. Lampre, L. Ruhlmann, *Appl. Catal. B Environ.* **2008**, *84*, 835–842.

[20] C. R. Graham, L. S. Ott, R. G. Finke, *Langmuir* **2009**, 25, 1327–1336.

[21] R. G. Finke, S. Özkar, *Coord. Chem. Rev.* **2004**, 248, 135–146.

[22] Y. Lin, R. G. Finke, *J. Am. Chem. Soc.* **1994**, *116*, 8335–8353.

[23] J. D. Aiken, R. G. Finke, *J. Am. Chem. Soc.* **1999**, *121*, 8803–8810.

[24] Y. Wang, A. Neyman, E. Arkhangelsky, V. Gitis, L. Meshi, I. A. Weinstock, *J. Am. Chem. Soc.* **2009**, *131*, 17412–17422.

[25] Y. Wang, O. Zeiri, V. Gitis, A. Neyman, I.A. Weinstock, *Inorganica Chim. Acta* **2010**, *363*, 4416–4420.

[26] M. Zhang, I. A. Weinstock, Y. Wang, *J. Clust. Sci.* **2014**, *25*, 771–779.

[27] A. Troupis, A. Hiskia, E. Papaconstantinou, *Angew. Chem.* **2002**, *114*, 1991–1993; *Angew. Chem., Int. Ed. Edngl.* **2002**, *41*, 1911–1914.

[28] G. Maayan, R. Neumann, *Catal. Lett.* **2008**, *123*, 41–45.

[29] G. Raveendra, A. Rajasekhar, M. Srinivas, P.S. Sai Prasad, N. Lingaiah, *Appl. Catal. A:*

Gen. **2016**, *520*, 105–113.

[30] M. Occhiuzzi, D. Cordischi, D. Gazzoli, M. Valigi, P. C. Heydorn, *Appl. Catal. A: Gen.* **2004**, *269*, 169–177.

[31] Y. Liu, S. Shrestha, W. E. Mustain, *ACS Catal.* **2012**, *2*, 456–463.

[32] I. J. Hsu, Y. C. Kimmel, Y. Dai, S. Chen, J. G. Chen, *J. Power Sources* **2012**, 199, 46–52.

[33] Y. A. Teterin, V. I. Nefedov, C. Ronneau, J. Vanbegin, J. Cara, I. O. Utkin, A. Y. Teterin, A. S. Nikitin, K. E. Ivanov, L. Vukcevic, et al., *Radiochemistry* **2001**, *43*, 604–609.

[34] Á. Vass, Z. Pászti, S. Bálint, P. Németh, G. P. Szíjjártó, A. Tompos, E. Tálas, *Mater. Res. Bull.* **2016**, *83*, 65–76.

[35] NIST X-ray Photoelectron Spectroscopy Database 20, Version 4.1 (National Institute of Standards and Technology, Gaithersburg, **2012**).

[36] S. Dugar, N. V. Izarova, S. S. Mal, R. Fu, H. Joo, U. Lee, N. S. Dalal, M. T. Pope, G. B. Jameson, U. Kortz, *New J. Chem.*, **2016**, *40*, 923–927.

[37] J. R. Khusnutdinova, P. Y. Zavalij, A. N. Vedernikov, *Organometallics* **2011**, *30*, 3392–3399.

[38] A. V. Sberegaeva, W. Liu, R. J. Nielsen, W. A. Goddard, A. V. Vedernikov, *J. Am. Chem. Soc.*, **2014**, *136*, 4761–4768

[39] N. Sun, A. Wu, Y. Yu, X. Gao, L. Zheng, *Chem. - A Eur. J.* **2019**, *25*, 6203–6211.

[40] N. Cheng, Y. Chen, X. Wu, Y. Liu, *Chem. Commun.* **2018**, *54*, 6284–6287.

[41] D. Radivojević, K. Seshan, L. Lefferts, *Appl. Catal. A Gen.* **2006**, *301*, 51–58.

[42] C. Dessal, L. Martínez, C. Maheu, T. Len, F. Morfin, J. L. Rousset, E. Puzenat, P. Afanasiev, M. Aouine, L. Soler, et al., *J. Catal.* **2019**, *375*, 155–163.

[43] Y. Zhu, T. Wang, T. Xu, Y. Li, C. Wang, *Appl. Surf. Sci.* **2019**, *464*, 36–42.

[44] X. Li, W. Bi, L. Zhang, S. Tao, W. Chu, Q. Zhang, Y. Luo, C. Wu, Y. Xie, *Adv. Mater.* **2016**, *28*, 2427–2431.

[45] N. Xiao, S. Li, S. Liu, B. Xu, Y. Li, Y. Gao, L. Ge, G. Lu, *Cuihua Xuebao/Chinese J. Catal.* **2019**, *40*, 352–361.

[46] C. Han, Y. Lu, J. Zhang, L. Ge, Y. Li, C. Chen, Y. Xin, L. Wu, S. Fang, *J. Mater. Chem. A* **2015**, *3*, 23274–23282.

[47] M. Ogawa, G. Ajayakumar, S. Masaoka, H. B. Kraatz, K. Sakai, *Chem. - A Eur. J.* **2011**, *17*, 1148–1162.

[48] M. Kobayashi, S. Masaoka, K. Sakai, *Angew. Chem.* **2012**, *30*, 7549–7552; *Angew. Chem., Int. Ed. Engl.* **2012**, *51*, 7431–7434.

[49] X. Liu, Y. Li, S. Peng, G. Lu, S. Li, *Int. J. Hydrogen Energy* **2012**, *37*, 12150–12157.

[50] X. Liu, Y. Li, S. Peng, G. Lu, S. Li, *Int. J. Hydrogen Energy* **2013**, *38*, 11709–11719.

[51] Y. Li, C. Xie, S. Peng, G. Lu, S. Li, *J. Mol. Catal. A Chem.* **2008**, *282*, 117–123.

[52] X. Liu, Y. Li, S. Peng, G. Lu, S. Li, *Photochem. Photobiol. Sci.* **2013**, *12*, 1903–1910.

[53] A. Tézé, G. Hervé, *Inorg. Synth.* **1990**, *27*, 88–92.

[54] A. Tézé, G. Hervé, *J. Inorg. Nucl. Chem.* **1977**, *39*, 999–1002.

[55] R. Ma, T. Wei, C. Zhao, *Huaxue Shiji/Chem. Reagents* **2011**, *33*, 307.